Food and Chemical Toxicology 133 (2019) 110720

Contents lists available at ScienceDirect

Food and Chemical Toxicology

journal homepage: www.elsevier.com/locate/foodchemtox

Glucose-regulated protein 75 in foodborne disease models induces renal tubular necrosis

Xuan Yang[a], Yijia Li[a], Lirong Zheng[a], Xiaoyun He[a], Yunbo Luo[a], Kunlun Huang[a,b,**], Wentao Xu[a,b,*]

[a] Beijing Advanced Innovation Center for Food Nutrition and Human Health, College of Food Science & Nutritional Engineering, China Agricultural University, Beijing, 100083, China
[b] Beijing Laboratory for Food Quality and Safety, Beijing, 100083, China

ARTICLE INFO

Keywords:
Grp75
Mitochondria
Kidney
Foodborne disease
Ochratoxin A

ABSTRACT

The incidence of kidney disease has increased rapidly in recent years. One major possible reason for this increase in nephrosis is from foodborne toxins. Since the mechanism of how foodborne toxins are involved in the process of nephrosis is largely unknown, the current study aims to establish a profile for how one of the major toxin threats, ochratoxin A (OTA), induce differential protein expression. In this proteomic study of rat kidneys, 75 kd glucose-regulated protein (Grp75) expression was found to be sensitized by a low concentration of OTA, but inhibited by high doses. In response to OTA, a decrease in Grp75 expression preceded the inhibition of mitochondrial Lon peptidase 1 (Lonp1). Using Grp75 knockdown cell line, it was shown that the inhibition of Grp75 promoted the secretion of kidney injury molecule 1 (Kim1), and suppressed Lonp1 expression in renal injury. Moreover, the acceleration of renal disease was associated with the consumption of Grp75. Our study suggests that the Grp75 protein may be valuable as both a treatment and biomarker for the foodborne diseases that induce renal tubular necrosis. The findings of this research are beneficial for the establishment of nutritional interventions, and the screening of therapeutic targets, in cases of nephrosis.

1. Introduction

Recent epidemiological studies have confirmed that the incidence of kidney failure and chronic kidney disease (CKD) has increased rapidly, resulting in a worldwide health crisis (Eckardt et al., 2013a; Levin et al., 2017). The global prevalence of CKD has risen to up to 10% (James et al., 2010; Zhang et al., 2016a, 2017). Diet and foodborne toxins are two common causes of kidney failure, with mycotoxins (Bol et al., 2016; Lunyera et al., 2016), heavy metals (Wanigasuriya et al., 2011) and pesticide residues (Siddarth et al., 2014) posing major threats to the pathogenesis and progression of acute or chronic kidney disease (Eckardt et al., 2013b). During the pathogenesis of kidney diseases, renal tubule cells, which are rich in mitochondria, cannot carry out their original functions, and cannot generate sufficient quantities of Adenosine triphosphate (ATP) to achieve the mass exchange of substances across kidney cells required to maintain sufficient renal function (Che et al., 2014). Moreover, there remain other, still unknown, mechanisms by which these toxic substances induce renal tubular necrosis, thus impeding identification and treatment.

Ochratoxin A (OTA) is one of the most abundant food-contaminating mycotoxins (Duarte et al., 2010; Peng et al., 2015; Pfohl-Leszkowicz and Manderville, 2007), and has been detected in the plasma and urine samples of Asian, European and African people (Clark and Snedeker, 2006; Coronel et al., 2011; Desalegn et al., 2011; Zaied et al., 2011), especially those with chronic interstitial nephropathy (Desalegn et al., 2011; Zaied et al., 2011). Furthermore, OTA has attracted considerable attention because of its carcinogenic, neurotoxic, teratogenic, immunogenic, and nephrotoxic properties (Reinsch et al., 2005), which is why it is widely used in practical disease model (Bui-Klimke and Wu, 2015). Kidneys are the main target organs of OTA-induced toxicity (World Health Organization, 2006). Pathologically, renal blood flow and the presence of a variety of transporters enable the active uptake and intracellular accumulation of high levels of OTA in the kidneys (Mally and Dekant, 2009), thus inducing CKD and renal cell carcinoma (Maisonneuve et al., 1999; Mally, 2012; NTP, 1989). Mitochondria are critical targets of OTA. Lower mitochondrial membrane potential, reactive oxygen species (ROS) bursting, protein synthesis inhibition and stress response induction are all consequences of OTA

* Corresponding author. College of Food Science and Nutritional Engineering, China Agricultural University, No. 17 Qinghua Donglu, Beijing, China.
** Corresponding author. College of Food Science and Nutritional Engineering, China Agricultural University, No. 17 Qinghua Donglu, Beijing, China.
E-mail addresses: hkl009@163.com (K. Huang), xuwentao@cau.edu.cn (W. Xu).

https://doi.org/10.1016/j.fct.2019.110720
Received 2 April 2019; Received in revised form 4 July 2019; Accepted 26 July 2019
Available online 29 July 2019
0278-6915/

toxicity (Shen et al., 2013). Moreover, it is clear that OTA-induced toxicity, caused by the expression of Kim1 (Qi et al., 2014b), pro-apoptotic proteins Bax (Zhang et al., 2016b) and Bad (Chopra et al., 2010), and apoptosis signal-regulating kinase1 (Liang et al., 2015) can aggravate kidney injury and induce renal cell death.

Heat shock proteins (HSPs) facilitate the formation of the secondary and tertiary structures of proteins, and assist with numerous reparative processes (Kampinga and Craig, 2010; Pockley, 2003). In kidney tissue, HSPs are an important part of the intracellular defense system, which operates physiologically and is activated by different types of cellular stress (Chebotareva et al., 2017). The various HSPs inside the cell provide stabilization for cellular structures, enhance cell resistance to apoptosis and necrosis, and preserve their potential for further regeneration. In the HSP70 family, HSP73 is located in renal tubular cells and participates in a protective response to the damaging components of proteinuria (Komatsuda et al., 1992), while HSP72 plays an important role in acute kidney injury (AKI) induced by renal ischemia in animals and humans (Guo et al., 2014). The HSP70 family has a wide spectrum of functions common to all chaperone proteins, including participation in shaping the structure of newly synthesized native proteins, restoration of partially denatured proteins, and degradation of irreversibly damaged protein molecules (Chebotareva et al., 2017). Moreover, HSP70 also limits pro-inflammatory NF-κB signaling in ischemic renal injury, by inhibiting the translocation of the NF-κB signaling protein p65 to the nucleus (Wang et al., 2011). A significant increase in intracellular HSP72 in tubular cells has been reported in patients with end-stage renal disease who are on dialysis, while the excretion of HSP70 is significantly elevated in the urine of patients with stages 4 and 5 CKD (Lebherz-Eichinger et al., 2012). Furthermore, increased renal cortical HSP70 content can lead to a decrease of blood urea nitrogen (BUN) levels in renal tubular lesions, thus suggesting improved animal survival (Wang et al., 2011). It is for these reasons that HSPs are believed to be promising targets for the development of new approaches to the treatment of kidney diseases (Chebotareva et al., 2017).

Grp75 (HSPA9 or mortalin), a mitochondrial inner membrane protein belonging to the HSP70 family (Mazkereth et al., 2016), was reported to be significantly inhibited in the renal cortex of 5/6 nephrectomized rats (Fedorova et al., 2013). Although Grp75 is considered a stress protein (Stacchiotti et al., 2006), its role in kidney injury is still unclear. In this assay, for the first time, we use a combination of OTA-induced subchronic acute nephrotoxicity models and a human renal tubular necrosis model to measure the changes in Grp75 expression in different degrees of kidney injury. We certified the function of Grp75 in the nephrotoxic process, thereby providing novel indicators of stress-induced kidney injury and establishing them for application to nutritional intervention.

2. Materials and methods

2.1. Animal handling

Experimental procedures involving animals were approved by the Ethics Committee (China Agricultural University, Beijing, PRC). The six-week-old male SPF F344 and Wistar rats used in this study were kept in accordance with institutional guidelines (Supervision and Testing Center for GMO Food Safety, Ministry of Agriculture, Beijing, China), with the license number SYXK (Beijing) 120001. In the subchronic toxicity experiments, the F344 rats were divided into three groups of six each, labelled C, L and H, and were housed three per cage at a controlled temperature of 22 ± 2 °C, a relative humidity of 40–70% and a 12-h light-dark cycle. Feed and sterilized water were consumed *ad libitum,* and rats were additionally gavaged with OTA doses (0, 70 or 210 μg/kg body weight) dissolved in corn oil (Aladdin, China) for 13 weeks (NTP, 1989). In the acute toxicity feeding experiment, the Wistar rats in groups C and A were each gavaged with corn oil OTA doses (4 mg/kg body weight) for 1 week (NTP, 1989). Body weights were recorded weekly. At the end of the experiment, the rats were anesthetized using chloral hydrate (6%, 5 ml/kg body weight). The kidney tissue was dissected quickly, then frozen in liquid nitrogen and stored at −80 °C. In addition, partial renal tissue was preserved in 4% polyoxymethylene (Aladdin, China) and used for immunohistochemical analysis.

Human renal tubular epithelial cells (HKC) were purchased from the national experimental cell resource sharing platform at Peking Union Medical College. The HKC cells were cultured in an 87% DMEM/F12 medium (Hyclone, USA), with 10% fetal bovine serum (Gibco, USA), 1% antibiotic: penicillin, streptomycin, amphotericin B, 100 units/mL (Gibco, USA), 1% non-essential amino acid (Hyclone, USA), and 1% glutamine (Sigma, USA).

2.2. Relative quantitative protein profiling and mass spectrometry

Total cell lysates were generated and protein quantitation performed, as described previously (Qi et al., 2014a). Considering that the texture of kidney is softer than that of liver, the ultrasonic time was shortened to 40 s at 4 °C. Isoelectric focusing (IEF) was performed in IPG strips (pH 4–7, 13 cm, GE Healthcare, USA) on a Multiphor III system (GE Healthcare, USA). The proteins were visualized with Coomassie Brilliant Blue R-250. Image digitization was performed with an image scanner (GE Healthcare, USA) in transmission mode. Image Master 2D 7.0 software (GE Healthcare, USA) was used in the gel analysis. Three independent experiments were conducted and a one-way ANOVA test ($p > 0.05$) was used to select the significant differentially abundant spots between groups.

For mass spectrometry, spot picking of interest was carried out with preparative gels and subjected to in-gel trypsin digestion, according to a previous study with minor modifications (Sun et al., 2007a). The peptide mass spectra were obtained with a MALDI-TOF/TOF mass spectrometer (4800 Proteomics-Analyzer, Applied Biosystems, USA), according to the previous method (Sun et al., 2007b). GPS Explorer™ software 3.6 (Applied Biosystems, USA), MASCOT (Matrix Science, http://www.matrixscience.com), and the NCBI rat database were used for peptide and protein identification.

2.3. Western blot analysis

Extracted proteins from each sample were loaded onto 12.5% Tricine-SDS-PAGE gels, transferred to a PVDF membrane (Millipore, Massachusetts, USA), blocked in 5% (wt/vol) skim milk in TBST (0.02 M Tris base, 0.14 M NaCl, 0.1% Tween 20, pH 7.4), and incubated with primary antibodies overnight at 4 °C before being further incubated with secondary antibodies conjugated with HRP. The following primary antibodies were used: rabbit Grp75 antibody (3593, CST, USA, 1:1000), rabbit Lonp1 antibody (15440, Proteintech, USA, 1:1000), rabbit Kim-1 antibody (ab78494, Abcam, USA, 1:1000), rabbit peroxiredoxin 2 antibody (46855, CST, USA, 1:1000) and rabbit β-actin antibody (aa128, Beyotime, China, 1:1000). Restore PLUS Western Blot Stripping Buffer (Thermo, Massachusetts, USA) and Super Signal West Pico chemiluminescent substrate (Sage Creation, Beijing, China) were used for coloration of the proteins. The total gray values of each band were digitized using BandScan V4.3. The relative expression level of each protein was normalized to a reference protein, and the resulting ratios in the control group were normalized to 1.

2.4. Immunohistochemistry

Kidney sections (5 μm) were prepared from formalin-fixed, paraffin-embedded tissue blocks and mounted onto glass slides. Sections were subsequently deparaffinized, rehydrated and washed in PBS. Antigen retrieval was performed using a 0.01 M citrate buffer (pH 6.0) boiled in a microwave oven for 20 min. Endogenous peroxidase activity was

blocked with 3% hydrogen peroxide for 30 min, while immunostaining was performed following the streptavidin–biotin–peroxidase complex method. Rabbit Grp75 antibody (3593, CST, USA, 1:50), rabbit YAP antibody (17074, CST, USA, 1:100), and rabbit β-catenin antibody (8480, CST, USA, 1:100) were applied as primary antibodies, before overnight incubation at 4 °C. Goat anti-rabbit (ZDR-5403) (Zsbio, China), 1:200, was applied as the biotinylated secondary antibody and incubated for 2 h at room temperature. Following incubation with streptavidin–HRP (Zymed, USA) for 2 h, the sections were developed using DAB (Sigma, USA) for 2 min, after which they were counterstained with hematoxylin (Beyotime, China), dehydrated and mounted in a neutral balsam (Beyotime, China). The images were captured with a fluorescent microscope (Olympus BX-51, Japan).

2.5. Cell viability assay

Cell viability was determined using Cell Counting Kit-8 (CCK-8) (Beyotime, China). 1×10^4 cells/well were seeded in a 96-well flat-bottomed plate for 24 h, after which the cells were washed once with PBS and then treated with concentrations of 0.25–50 μM OTA in 5 independent experiments over periods of 24 h, 48 h or 72 h. 10 μL of water-soluble-tetrazolium salt-8 dye were added to each well, then incubated at 37 °C for 2 h. The absorbance values were determined at 450 nm using a microplate reader (Thermo, USA).

2.6. Knockdown of Grp75 by RNA interference

HKC were seeded at a density of 1×10^6 cells/well in 6-well plates. When the cell density was more than 60%, cells were transferred to fresh serum-free medium 1 h before transfection with either Grp75 siRNA (sc-35520, Santa Cruz Biotechnology, USA) or scrambled siRNA diluted with a DMEM/F12 medium. Lipofectamine 3000 transfection reagent was diluted with the DMEM/F12 culture medium, prepared according to instructions, then incubated at room temperature for 5 min. Lipofectamine 3000 working liquid was added to the siRNA diluent by dropper, incubated at room temperature for 20 min, then mixed into the cell culture medium without antibiotic and serum. After being cultured for 20 h, the protein was extracted and a Western blot was used to detect the interference efficiency.

2.7. Immunofluorescence

Sterile coverslips were placed at the bottom of 6-well plates before inoculation of cells with different treatments, to complete the cell climbing process. After removal of the supernatant, 2 mL 4% polyformaldehyde was added to each well and left for 10 min. Then, PBS with 0.5% Triton was added to each well for 15 min. After PBS washing, 1% BSA was added for a further 30 min. The following primary antibodies were used: rabbit Grp75 antibody (3593, CST, USA, 1:100), rabbit Kim-1 antibody (ab78494, Abcam, USA, 1:100), mouse a-SMA antibody (ab7817, Abcam, USA, 1:200), and mouse 8-hydroxyguanosine antibody (ab26842, Abcam, USA, 1:200). 5 μg/mL DAPI (ab104193, Abcam, USA) was used for mounting, before storage in dark conditions at 4 °C. A Zeiss 880 laser confocal microscope (Carl Zeiss, GER) was used to perform the immunofluorescence imaging with an Airscan laser.

2.8. Statistics

The data is presented as the average, with standard deviation, of three parallel experiments. The data from the different treatments was subjected to a one-way analysis of variance (ANOVA) and the means were compared using Duncan's multiple range test. Differences of less than 0.05 were considered significant for p-values.

3. Results

3.1. Protein expression profiles show OTA-induced subchronic renal injury in rats

After the administration of OTA, the body masses of high-OTA-dose rats were reduced by approximately 7% ($p < 0.05$) at 9 and 10 weeks, while, in a postmortem analysis at 13 weeks, their kidney weights were markedly decreased in comparison to those of the control group (Qi et al., 2014a). Pathologic changes in the kidneys of rats treated with OTA for 13 weeks included mild deep vein cortical expansion, renal tissue edema, renal duct epithelial cell necrosis, and renal tubular epithelial cell fall-off in the renal tissues (Dai et al., 2014). Protein samples for 2-DE obtained from detached renal tissues after 13 weeks' OTA administration, were 0 μg/kg in the C (control) group, 70 μg/kg in the M (mid-dose) group, and 210 μg/kg in the H (high-dose) group. Changes in the abundance of proteins were measured and compared between these three samples in three independent replicate calculations. Analysis of the 2-DE pattern revealed that most protein spots on the gel had an acidic pI value in the range of pH 4–7 and a molecular mass of between 15 kDa and 80 kDa. Approximately 1600 protein spots could be detected on the 2-D gel, excluding very faint spots and those with undefined shapes and areas. Quantitative analysis of the spot intensity, through the integration of the staining signal for each gel and image analysis, revealed that the levels of 110 of the resolved proteins changed in an OTA-dependent manner (ratio > 1.5) in three independent experiments (Supplementary Table 1, Supplementary Fig. 1). The 70 protein spots that showed a relatively high abundance were analyzed using MALDI-TOF/TOF MS/MS, as shown in Fig. 1A. The results of this analysis were submitted to the MASCOT search engine for database searching and are summarized in Supplementary Table 1 and Fig. 1B. Ultimately, 47 spots, representing 42 different proteins, were identified with significant Mascot scores ($P < 0.05$). It is noteworthy that five of the protein spots were identified as belonging to the same protein. The location of these spots in the gels differed in molecular mass and pI, indicating that they might be catabolites or have different post-translational modifications. Protein profiles from the three groups of kidneys were catalogued according to their cellular components, molecular functions and biological processes, according to the WEGO database (Fig. 1C). Analysis of the GO pathways, using Panther, indicated that the differential proteins are mainly involved in energy metabolism, antioxidation, and apoptosis related pathways (Fig. 1D), while the analysis of GO molecular functions indicated that the differential proteins are mainly involved in catalytic activity, transcription factors and antioxidation pathways (Fig. 1E).

3.2. Grp75 participates in renal injury regulation in an OTA-induced rat toxicity model

In our proteomic study of OTA-induced nephrotoxicity, the expression of Grp75 (Hspa9, gi 410110929), was regulated by OTA exposure. Our quantitative verification showed that in the OTA (L) group the expression of Grp75 protein was up-regulated 2.1 times more than that of the control group, while in the OTA (H) group the expression of Grp75 was down-regulated 0.35 times more than in the OTA (L) group (Fig. 2A). These findings are consistent with the proteomic results. Moreover, immunohistochemistry showed that Grp75 was mainly concentrated in the renal tubular epithelial cells and Grp75 expression increased in the OTA (L) group, but decreased in the higher concentrations of the OTA (H) treatment group (Fig. 2B). In addition, the expression of peroxiredoxin 2 was validated in the same experiment (Fig. 2C). According to the proteomic and Western blot results, OTA inhibited the expression of peroxidase 2 in renal tissue, suggesting that OTA can increase the degree of peroxidation in this period. This is the first time in which OTA-induced toxicology has been shown to be mediated by peroxidase 2.

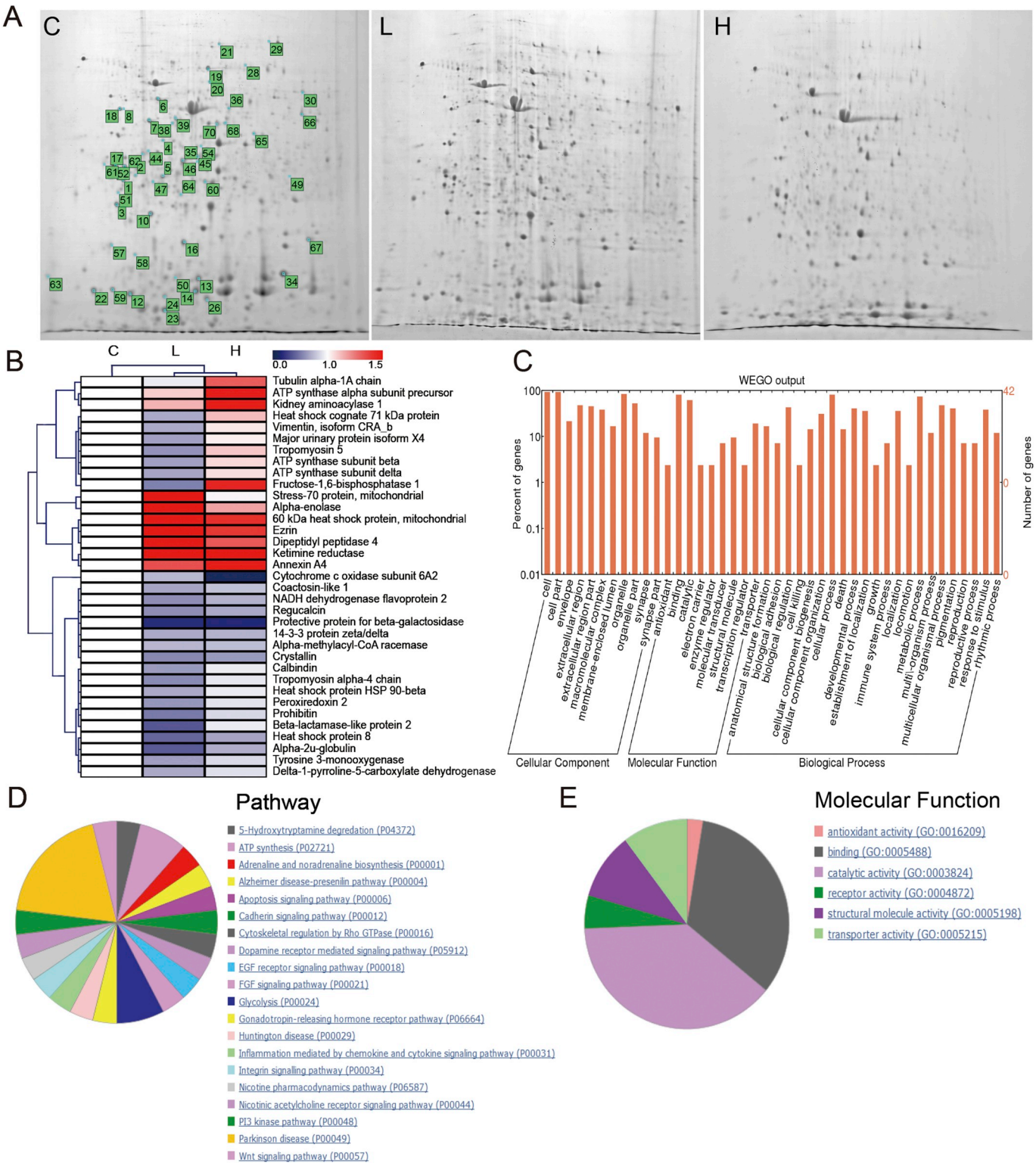

Fig. 1. Proteomics analysis of OTA-induced hepatotoxicity in rats. (A) After 3 months of OTA treatment, the liver protein profiles were analyzed by two-dimensional electrophoresis. Total protein (400 μg) was separated on 2D gels (pH 4–7 NL) and stained with colloidal Coomassie Brilliant Blue R-250; (B) The fold change of differential expression proteins in kidney; (C) WEGO analysis of differentially expressed proteins; (D) Pathway enrichment analysis of differentially expressed proteins; (E) Molecular function analysis of differentially expressed proteins. (For interpretation of the references to color in this figure legend, the reader is referred to the Web version of this article.)

3.3. Expression of Grp75 in renal injury regulation in an acute OTA-toxicity-induced rat model

In the rat model, after one weeks' gavage treatment with 4 mg/kg body weight OTA, the pathological features of acute renal injury were confirmed. Furthermore, the renal injury related markers clusterin (*Clu*), neutrophil gelatinase-associated lipocalin 2 (*Lcn2*) and Kim-1 were also up-regulated (Zhu et al., 2016). In this study, we showed that

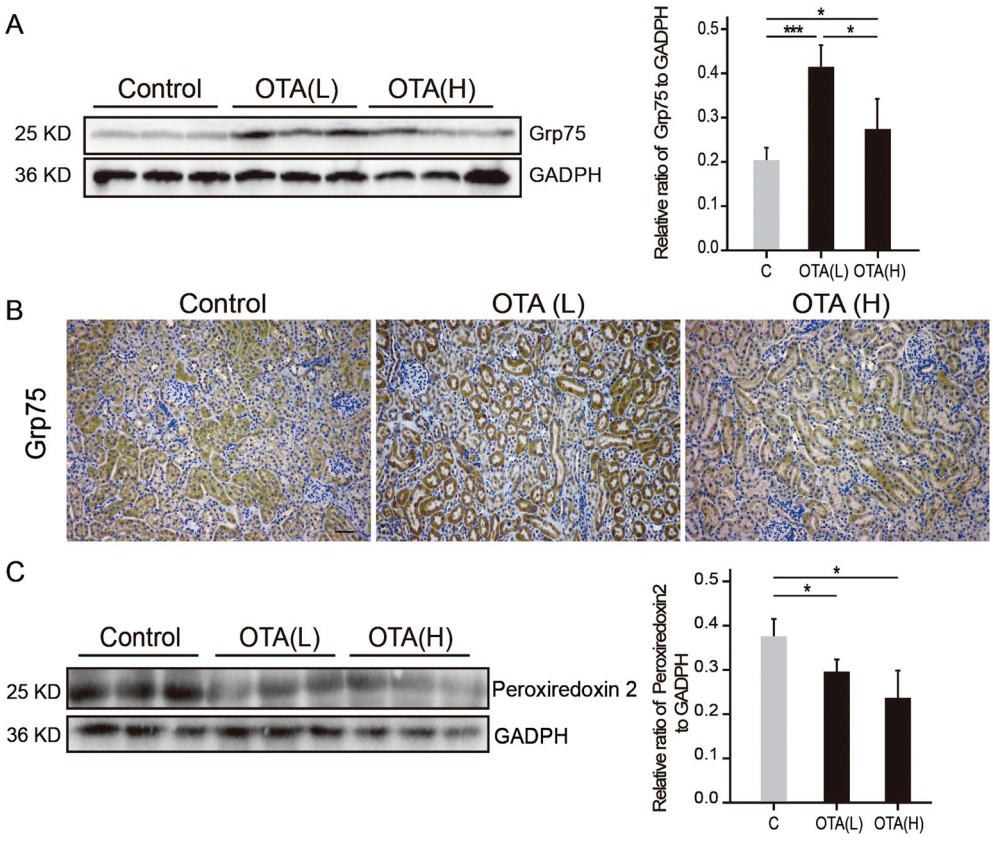

Fig. 2. Quantitative analysis of proteomic differential proteins in rat kidney under 3-months' OTA treatment. (A) Effects of different doses of OTA treatment on the expression of Grp75 in rat kidneys, and quantitative analysis; (B) Immunohistochemical analysis of Grp75 expression in rat kidneys; (C) Effect of different doses of OTA treatments on the expression of peroxiredoxin2 protein in rat kidney, and quantitative analysis. n = 5–6 per group. Scale bars = 100 mm. Error bars represent means ± SEM. "*" indicates a significant difference ($P < 0.05$), and "***" indicates a significant difference ($P < 0.005$) compared with other groups.

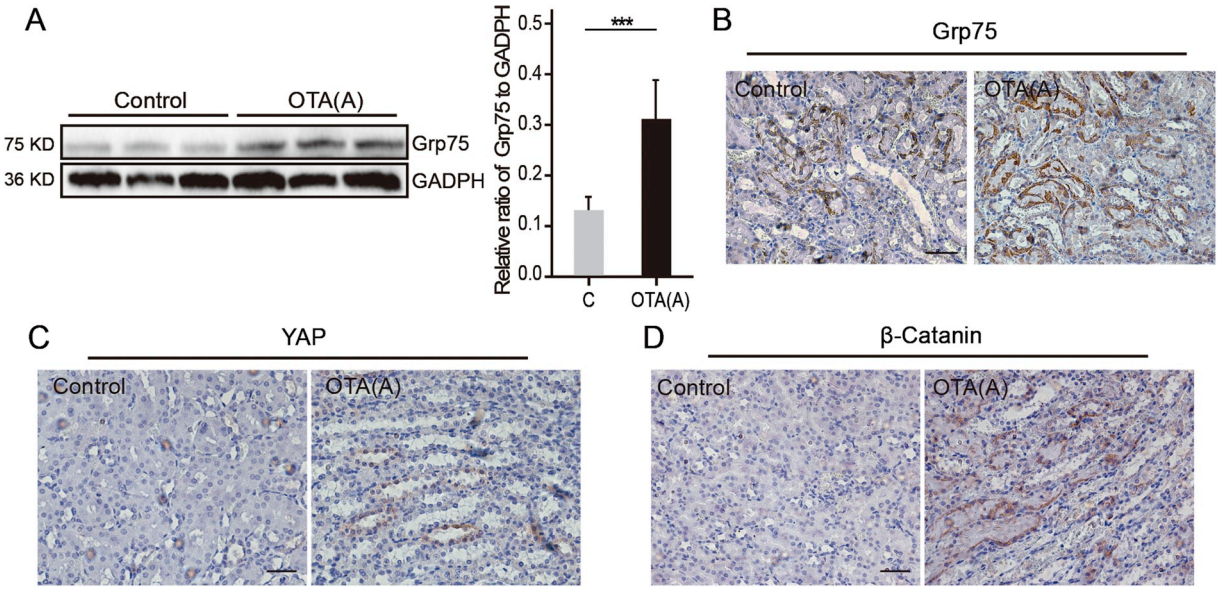

Fig. 3. Quantitative analysis of proteomic differential proteins in rat kidney under 7-days' OTA treatment. (A) Effects of OTA treatment on the expression of Grp75 in rat kidneys, and quantitative analysis; Immunohistochemical analysis of (B) Grp75, (C) YAP, (D) β-catenin protein expression in rat kidneys. Scale bars = 100 mm. Error bars represent means ± SEM. "***" indicates a significant difference ($P < 0.005$) compared with other groups.

the expression of Grp75 was significantly up-regulated in our OTA-induced acute renal injury model (Fig. 3A), a finding that was further confirmed by immunohistochemistry (Fig. 3B). The up-regulation of Grp75 in kidneys with subchronic and acute toxicity, and depression in the higher dose and long-term OTA gavage groups, suggests that Grp75 might be stressed by toxin induced-CKD, and thus attenuated by any increase in the degree of injury. Wnt/β-catenin and Hippo/YAP are the classical pathways of tumorigenesis and cell proliferation (Oudhoff et al., 2016). In rats undergoing OTA-induced acute renal injury, the YAP and β-catenin signals were found by immunohistochemistry (Fig. 3C and D). The activation of Grp75 was simultaneously detected with the production of YAP and β-catenin signals, suggesting that up-regulation of Grp75 may be associated with the identification or mitigation of renal cell abnormalities.

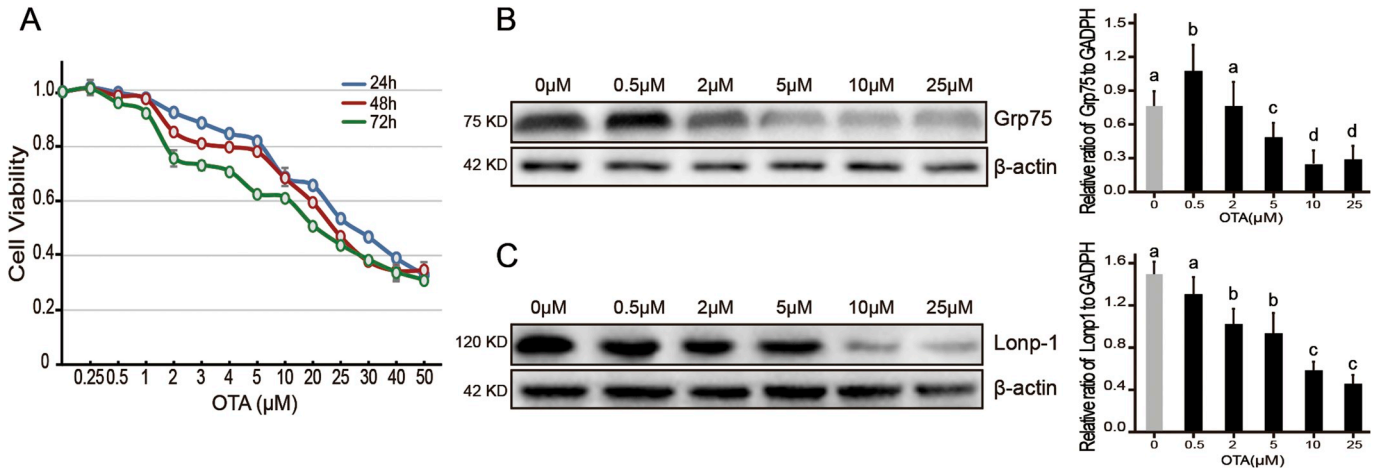

Fig. 4. Quantitative analysis of OTA-induced protein expression changes in HKC cells. (A) Effect of different concentrations of OTA on the viability of HKC cells; (B) Different doses of OTA on the expression of Grp75 in HKC cells, and quantitative analysis; (C) Effects of different doses of OTA on the expression of Lonp-1 in HKC cells, and quantitative analysis. The values are the mean ± SD of three independent experiments. Different characters indicate significant differences between the comparative groups ($p < 0.05$).

3.4. Grp75 is suppressed by high concentrations of OTA, and is preceded by Lonp1 suppression in human renal epithelial cells

In *vitro*, human kidney epithelial cell lines (HKC) were used to show the expression of Grp75 under OTA treatment. Curves of HKC cell viability under 24 h, 48 h, and 72 h conditions with OTA treatment are shown in Fig. 4A. The results showed that in the 24-h treatment groups, the semi-lethal dose of OTA to HKC was 28 μM, while in the 48-h treatment the dose was 24 μM and in the 72-h treatment it was 16 μM. Considering that the 72 h treatment resulted in the highest mortality, and that 24 h and 48 h treatments are the most widely used cytotoxicity evaluation models, a time point of 48 h was selected in which to study the relationship between the concentration gradient of OTA and the expression of Grp75 (Blazer-Yost et al., 2005; Raghubeer et al., 2015). The results showed that, under normal conditions, intracellular Grp75 was expressed to a certain extent, suggesting that this protein may not promote the occurrence of apoptosis. Under conditions of 0.5 μM OTA treatment for 48 h, the expression of Grp75 protein was up-regulated by 1.3 times; however, when the concentration of OTA was higher than 2 μM, the expression of Grp75 was suppressed by the increased concentration of OTA (Fig. 4B). This suggests that Grp75 may be involved in the response of renal tubular epithelial cells to OTA stress.

Lonp1 is involved in regulating the mitochondrial redox balance, maintaining mtDNA homeostasis and protecting cells from oxidative stress (Pinti et al., 2015). In this study it was found that the expression of Lonp1 was significantly inhibited after OTA-induced HKC cell viability was decreased by 30% (Fig. 4C), while the expression of Grp75 was significantly inhibited after cell viability was decreased by 20%. This suggests that, in HKC cells, the response of Grp75 to OTA may be more sensitive than Lonp1. Taking into account the results of proteomics, it is possible that OTA may inhibit mitochondrial respiratory metabolism in renal cells, and that the decrease of Grp75 expression is probably related to mitochondrial respiratory metabolism.

3.5. Knock-down of Grp75 inhibits the expression of Lonp1 and promotes the expression of Kim-1 in renal tubular epithelial cells exposed to OTA

To further verify the role of Grp75 in the process of renal injury, the Grp75 knockdown cell lines were established and exposed to OTA environment. After 24 h of siRNA interference, the expression of Grp75 in HKC cells was found to be knocked down (Fig. 5A), with an interference efficiency of 60%. Subsequently, 10 μM OTA was used to treat cell lines for 24 h, after which the cells were immobilized and the protein was extracted. Immunofluorescence staining of Grp75 and smooth muscle actin (a-SMA) indicated that the cytoskeleton showed a certain contractionary trend after OTA treatment, and the expression of Grp75 was inhibited in the treatment groups (Fig. 5B). Quantitative protein results showed that OTA could activate the expression of Kim-1, a marker protein for tubular kidney injury (Nielsen et al., 2009). Moreover, Kim-1 expression was further enhanced in the Grp75 knock-down cell lines under OTA treatment (Fig. 5C), suggesting that Grp75 may be involved in the protection of HKC cells. Additionally, Lonp1 has been used as a marker to evaluate the degree of damage to mitochondria (Ngo and Davies, 2007). Under Grp75 knockdown, the expression of Lonp1 was decreased, but it was accentuated by OTA treatment (Fig. 5D). This result reveals that the inhibition of Lonp1 by OTA is medicated by Grp75, while the consumption of Grp75 accelerates the occurrence of mitochondrial damage.

In addition to the above findings, 8-hydroxy-2-deoxyguanosine (8-OHdG), which is a classic biomarker of oxidative DNA damage (Wu et al., 2004), was used in a preliminary evaluation of whether Grp75 participates in the OTA-induced DNA damage process. Immunofluorescence showed that OTA has a tendency to promote the generation of 8-OHdG in HKC cells; however, in this case, no significant difference was found in the expression of 8-OHdG in the Grp75 interference experiment (Fig. 5E and F).

4. Discussion

Mitochondria are important organelles that maintain the normal operation of metabolic cellular pathways, but they are vulnerable to oxidative damage (Goldenthal and Marin-Garcia, 2004). Previous studies have shown that OTA interferes with the function of mitochondrial electron transport chains in cells, and induces mitochondrial dysfunction (Musicco et al., 2011). Moreover, OTA exposure is a proven foodborne toxin that induces a kidney injury model, reducing ATP generation by inhibiting the voltage-dependent anion-selective channel protein, and thereby disturbing energy metabolism (Abu-Hamad et al., 2006) and inducing premature senescence (Yang et al., 2017), renal lipotoxicity and nephrosis (Yang et al., 2019). The complete protein expression profile of OTA-induced nephrotoxicity highlights the important status of energy metabolism and mitochondrial quality control systems in the occurrence and development of kidney diseases, and provides evidence for the prevention and treatment of mycotoxin-induced mitochondrial damage in the kidney.

The maintenance of renal function requires the coordination of

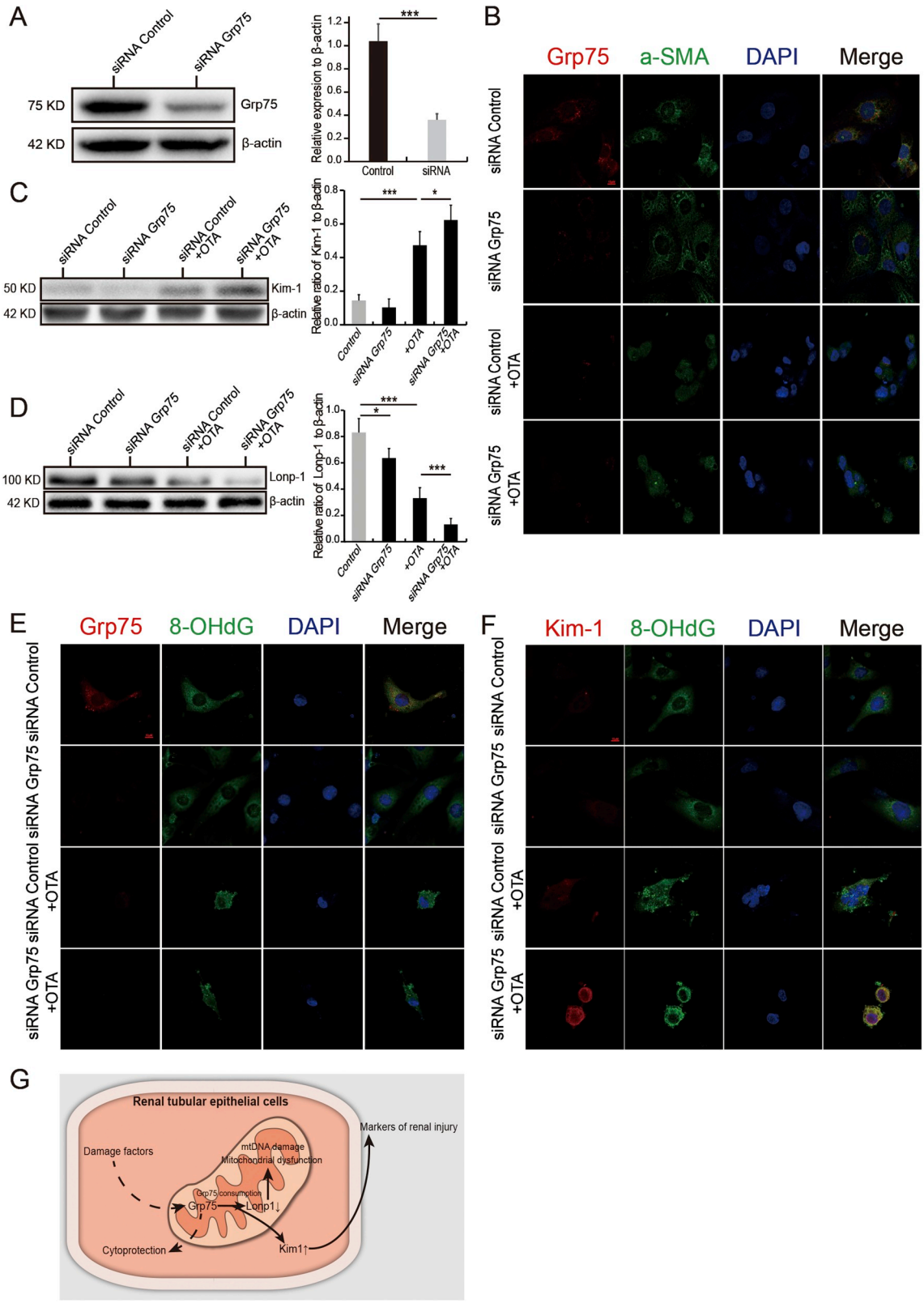

Fig. 5. The effect of Grp75 knock-down on the expression of Kim-1 and 8-OHdG in HKC cells. (A) Expression of Grp75 after siRNA knockdown, and quantitative analysis; After Grp75 knockdown, HKC cells were treated with 25 μM OTA for 24h, (B) Immunofluorescence analysis of the expression of Grp75; (C) Expression of Kim-1 protein and quantitative analysis; (D) Expression of Kim-1 protein and quantitative analysis; (E) Immunofluorescence analysis of the relationship between the expression of Grp75 and 8-OHdG; (F) Immunofluorescence analysis of the relationship between the expression of Kim-1 and 8-OHdG; (G) Schematic diagram. Scale bars = 10 μm. Error bars represent mean ± SEM. "*" indicates a significant difference ($P < 0.05$), "***" indicates a significant difference ($P < 0.005$) between the comparative groups.

multiple organelles in renal cells (Munusamy et al., 2015). Mitochondrial damage and genomic instability trigger tubular endoplasmic reticulum extension to promote apoptosis by facilitating ER-mitochondria signaling (Zheng et al., 2018), and the suppression of Grp75 has been proven to drive this trend and aggravate both ATP depletion and the subsequent mitochondrial dysfunction (Honrath et al., 2018). Suppression of Grp75 also leads to the depolarization of mitochondria in the membrane, reduction of oxygen consumption, increase in extracellular acidification, and oxidative stress, all of which disrupt mitochondrial energy metabolism by the activation of the Raf-MEK-ERK pathway (Raf-mitogen-activated kinase/extracellular signal-related kinase pathway) and, ultimately, accelerate cell death (Starenki et al., 2015). Furthermore, Lonp1, which plays important roles in alleviating oxidative stress and maintaining mtDNA stability (Zhang et al., 2014), highlighting the relationship between Grp75 and mitochondrial protection mechanisms. One is that, in our Grp75 knockdown model, under the toxin-induced stress conditions, the suppression of Grp75 enhances the suppression of Lonp1. This suggests that there may not be a direct bond between Grp75 in the inner mitochondrial membrane and Lonp1 in the mitochondrial matrix, but rather, Grp75 is probably a receptor that controls the degradation or synthesis of Lonp1. On the other hand, in our experiments on OTA exposure, Grp75 expression decreased before Lonp1, thus confirming that Grp75 is an earlier indicator than Lonp1 of the different degrees of mitochondrial damage. The second noteworthy consideration is that Lonp1 also improves the protein synthesis process in mitochondria (Ngo and Davies, 2007). The Grp75-Lonp1 mediated pathway may also reduce protein synthesis (Zanic-Grubisic et al., 2000), thereby destroying the balanced environment of mitochondria and increasing mtDNA mutation (Mutlu, 2012). It is worth noting that, in both our in vivo and in vitro models, we don't find that Lonp1 is suppressed in our treatment groups with less than 5 μM OTA. But when cell viability was decreased more than 20%, the expression of Lonp1 was suppressed significantly. This also indicates that the occurrence of mtDNA mutations may require the accumulation of a certain dose of toxin. This is illustrated in the schematic diagram shown in Fig. 5G.

The primary excretory organs in the human body are the kidneys, ureters and urinary bladder, all of which are involved in the creation and expulsion of urine. Urine contains high concentrations of both endogenous and exogenous toxins and viruses (Tan et al., 2017), which means kidneys must have a certain immunity to injury. Grp75 has been shown to cooperate with HSP90 family proteins in their resistance to endogenous and exogenous cell damage (Rozenberg et al., 2018), and to enhance the protection of cells from viral infection and cell lysis (Ray et al., 2014). Therefore, we suggest that the maintenance of Grp75 expression is necessary to avoid nephritis, and the decrease of Grp75 in renal tubular epithelial cells may also reduce renal cell immunity.

In the course of cancer development, Grp75 has been found to induce the expression of the Bcl-2 family protein, regulating p53, E2F-1, p21 and p27 signaling to suppress the cell cycle, thereby inhibiting the growth of carcinoma cells and significantly decreasing the genomic rearrangements made during the transfection process (Starenki et al., 2015). Therefore, excessive suppression of Grp75 could be a manifestation of OTA carcinogenicity in the kidney.

5. Conclusion

This study examined the protein expression profile of rat kidney under OTA treatment. The results show that OTA can significantly inhibit the expression of energy metabolism related proteins and can activate the expression of apoptosis related proteins in the kidney. Expression of Grp75, an HSP family member, is responsive to the concentration of nephrotoxic factors. Here, its expression in renal cells was first increased and then gradually suppressed with increasing doses of the nephrotoxic inducer OTA. The dosage relationship between Grp75 and OTA was also established in HKC cells. Furthermore, the results confirm that Grp75 responds earlier to risk factors for kidney damage than Lonp1, which is beneficial for kidney injury protection. Therefore, it may be concluded that Grp75 offers great potential as a new target for screening renal injury treatment drugs and nutrients, and a newly identified target for renal toxicity evaluation and nephrotoxic processes.

Acknowledgments

This work was supported by the National GMO Cultivation Major Project of New Varieties (2016ZX08011-005), China. We sincerely thank Siwen Zhao for her assistance with the confocal microscope at the Institute of Plant Protection, Chinese Academy of Agricultural Sciences. We also thank Jingli Li for her assistance with mass spectrometry analysis at the National Institute of Biological Sciences, Beijing, and Haoshu Luo for his assistance with RNA transfection reagent at the College of Biological Sciences, China Agricultural University.

Appendix A. Supplementary data

Supplementary data to this article can be found online at https://doi.org/10.1016/j.fct.2019.110720.

Author contributions

X. Yang and W. T. Xu designed research; X. Yang analyzed data; X. Yang, L. R. Zheng and Yijia Li performed research; X. Yang wrote the paper; K. L. Huang, Y. B. Luo and X. Y. He contributed new reagents or analytic tools.

Conflicts of interest

The authors declare that there are no conflicts of interest.

References

Abu-Hamad, S., Sivan, S., Shoshan-Barmatz, V., 2006. The expression level of the voltage-dependent anion channel controls life and death of the cell. Proc. Natl. Acad. Sci. U.S.A. 103, 5787–5792.

Blazer-Yost, B.L., West, T.A., Stack, J., Peck, K., Lahr, T.F., Gekle, M., 2005. Effect of the mycotoxin, ochratoxin A, on hormone-stimulated ion transport in a cultured cell model of the renal principal cell. Pflugers Arch. Eur. J. Phy. 450, 53–60.

Bol, E.K., Araujo, L., Veras, F.F., Welke, J.E., 2016. Estimated exposure to zearalenone, ochratoxin A and aflatoxin B1 through the consume of bakery products and pasta considering effects of food processing. Food Chem. Toxicol.: Int. J. Pub. Br. Ind. Biol. Res. Assoc. 89, 85–91.

Bui-Klimke, T.R., Wu, F., 2015. Ochratoxin A and human health risk: a review of the evidence. Crit. Rev. Food Sci. Nutr. 55, 1860–1869.

Che, R.C., Yuan, Y.G., Huang, S.M., Zhang, A.H., 2014. Mitochondrial dysfunction in the pathophysiology of renal diseases. Am. J. Physiol. Renal. 306, F367–F378.

Chebotareva, N., Bobkova, I., Shilov, E., 2017. Heat shock proteins and kidney disease: perspectives of HSP therapy. Cell Stress & Chaperones 22, 319–343.

Chopra, M., Link, P., Michels, C., Schrenk, D., 2010. Characterization of ochratoxin A-induced apoptosis in primary rat hepatocytes. Cell Biol. Toxicol. 26, 239–254.

Clark, H.A., Snedeker, S.M., 2006. Ochratoxin A: its cancer risk and potential for exposure. J. Toxicol. Environ. Health B 9, 265–296.

Coronel, M.B., Marin, S., Tarrago, M., Cano-Sancho, G., Ramos, A.J., Sanchis, V., 2011. Ochratoxin A and its metabolite ochratoxin alpha in urine and assessment of the exposure of inhabitants of Lleida, Spain. Food Chem. Toxicol. 49, 1436–1442.

Dai, Q., Zhao, J., Qi, X.Z., Xu, W.T., He, X.Y., Guo, M.Z., Dweep, H., Cheng, W.H., Luo, Y.B., Xia, K., Gretz, N., Huang, K.L., 2014. MicroRNA profiling of rats with ochratoxin A nephrotoxicity. BMC Genomics 15.

Desalegn, B., Nanayakkara, S., Harada, K.H., Hitomi, T., Chandrajith, R., Karunaratne, U., Abeysekera, T., Koizumi, A., 2011. Mycotoxin detection in urine samples from patients with chronic kidney disease of uncertain etiology in Sri Lanka. Bull. Environ. Contam. Toxicol. 87, 6–10.

Duarte, S.C., Pena, A., Lino, C.M., 2010. A review on ochratoxin A occurrence and effects of processing of cereal and cereal derived food products. Food Microbiol. 27, 187–198.

Eckardt, K.U., Coresh, J., Devuyst, O., Johnson, R.J., Kottgen, A., Levey, A.S., Levin, A., 2013a. Evolving importance of kidney disease: from subspecialty to global health burden. Lancet 382, 158–169.

Eckardt, K.U., Coresh, J., Devuyst, O., Johnson, R.J., Kottgen, A., Levey, A.S., Levin, A., 2013b. Evolving importance of kidney disease: from subspecialty to global health burden. Lancet 382, 158–169.

Fedorova, L.V., Tamirisa, A., Kennedy, D.J., Haller, S.T., Budnyy, G., Shapiro, J.I., Malhotra, D., 2013. Mitochondrial impairment in the five-sixth nephrectomy model of chronic renal failure: proteomic approach. BMC Nephrol. 14.
Goldenthal, M.J., Marin-Garcia, J., 2004. Mitochondrial signaling pathways: a receiver/integrator organelle. Mol. Cell. Biochem. 262, 1–16.
Guo, Q.M., Du, X.F., Zhao, Y.L., Zhang, D., Yue, L.H., Wang, Z.X., 2014. Ischemic post-conditioning prevents renal ischemia reperfusion injury through the induction of heat shock proteins in rats. Mol. Med. Rep. 10, 2875–2881.
Honrath, B., Culmsee, C., Dolga, A.M., 2018. One protein, different cell fate: the differential outcome of depleting GRP75 during oxidative stress in neurons. Cell Death Dis. 9, 32.
James, M.T., Hemmelgarn, B.R., Tonelli, M., 2010. Early recognition and prevention of chronic kidney disease (vol 375, pg 1296, 2010). Lancet 376 162-162.
Kampinga, H.H., Craig, E.A., 2010. The HSP70 chaperone machinery: J proteins as drivers of functional specificity (vol 11, pg 579, 2010). Nat. Rev. Mol. Cell Biol. 11.
Komatsuda, A., Wakui, H., Imai, H., Nakamoto, Y., Miura, A.B., Itoh, H., Tashima, Y., 1992. Renal localization of the constitutive 73-kda heat-shock protein in normal and Pan rats. Kidney Int. 41, 1204–1212.
Lebherz-Eichinger, D., Ankersmit, H.J., Hacker, S., Hetz, H., Kimberger, O., Schmidt, E.M., Reiter, T., Horl, W.H., Haas, M., Krenn, C.G., Roth, G.A., 2012. HSP27 and HSP70 serum and urine levels in patients suffering from chronic kidney disease. Clin. Chim. Acta 413, 282–286.
Levin, A., Tonelli, M., Bonventre, J., Coresh, J., Donner, J.A., Fogo, A.B., Fox, C.S., Gansevoort, R.T., Heerspink, H.J.L., Jardine, M., Kasiske, B., Kottgen, A., Kretzler, M., Levey, A.S., Luyckx, V.A., Mehta, R., Moe, O., Obrador, G., Pannu, N., Parikh, C.R., Perkovic, V., Pollock, C., Stenvinkel, P., Tuttle, K.R., Wheeler, D.C., Eckardt, K.U., I.S.N.G.K.H.S. participants, 2017. Global kidney health 2017 and beyond: a roadmap for closing gaps in care, research, and policy. Lancet 390, 1888–1917.
Liang, R., Shen, X.L., Zhang, B.Y., Li, Y.Z., Xu, W.T., Zhao, C.H., Luo, Y.B., Huang, K.L., 2015. Apoptosis signal-regulating kinase 1 promotes ochratoxin A-induced renal cytotoxicity. Sci. Rep. 5.
Lunyera, J., Mohottige, D., Von Isenburg, M., Jeuland, M., Patel, U.D., Stanifer, J.W., 2016. CKD of uncertain etiology: a systematic review. Clin. J. Am. Soc. Nephrol. : CJASN 11, 379–385.
Maisonneuve, P., Agodoa, L., Gellert, R., Stewart, J.H., Buccianti, G., Lowenfels, A.B., Wolfe, R.A., Jones, E., Disney, A.P.S., Briggs, D., McCredie, M., Boyle, P., 1999. Cancer in patients on dialysis for end-stage renal disease: an international collaborative study. Lancet 354, 93–99.
Mally, A., 2012. Ochratoxin a and mitotic disruption: mode of action analysis of renal tumor formation by ochratoxin a. Toxicol. Sci. 127, 315–330.
Mally, A., Dekant, W., 2009. Mycotoxins and the kidney: modes of action for renal tumor formation by ochratoxin A in rodents. Mol. Nutr. Food Res. 53, 467–478.
Mazkereth, N., Rocca, F., Schubert, J.R., Geisler, C., Hillman, Y., Egner, A., Fishelson, Z., 2016. Complement triggers relocation of Mortalin/GRP75 from mitochondria to the plasma membrane. Immunobiology 221, 1395–1406.
Munusamy, S., do Carmo, J.M., Hosler, J.P., Hall, J.E., 2015. Obesity-induced changes in kidney mitochondria and endoplasmic reticulum in the presence or absence of leptin. Am. J. Physiol. Renal. Physiol. 309, F731–F743.
Musicco, C., Capelli, V., Pesce, V., Timperio, A.M., Calvani, M., Mosconi, L., Cantatore, P., Gadaleta, M.N., 2011. Rat liver mitochondrial proteome: changes associated with aging and acetyl-L-carnitine treatment. J. Proteom. 74, 2536–2547.
Mutlu, A.G., 2012. Increase in mitochondrial DNA copy number in response to ochratoxin A and methanol-induced mitochondrial DNA damage in Drosophila. Bull. Environ. Contam. Toxicol. 89, 1129–1132.
Ngo, J.K., Davies, K.J., 2007. Importance of the lon protease in mitochondrial maintenance and the significance of declining lon in aging. Ann. N. Y. Acad. Sci. 1119, 78–87.
Nielsen, S.E., Schjoedt, K.J., Astrup, A.S., Tarnow, L., Lajer, M., Hansen, P.R., Parving, H.H., Rossing, P., 2009. Kidney injury molecule 1 (KIM1) and neutrophil gelatinase-associated lipocalin (NGAL) as markers of tubular kidney injury in type 1 diabetic patients. Diabetologia 52 S412-S412.
NTP, 1989. Toxicology and carcinogenesis studies of ochratoxin A (cas no. 303-47-9) in F344/N Rats (Gavage Studies). Natl. Toxicol. Program Tech. Rep. Ser. 358, 142.
Oudhoff, M.J., Braam, M.J.S., Freeman, S.A., Wong, D., Rattray, D.G., Wang, J., Antignano, F., Snyder, K., Refaeli, I., Hughes, M.R., McNagny, K.M., Gold, M.R., Arrowsmith, C.H., Sato, T., Rossi, F.M.V., Tatlock, J.H., Owen, D.R., Brown, P.J., Zaph, C., 2016. SETD7 controls intestinal regeneration and tumorigenesis by regulating wnt/beta-catenin and Hippo/YAP signaling. Dev. Cell 37, 47–57.
Peng, C.H., Wang, L., An, F.P., Zhang, L., Wang, Y.C., Li, S.R., Wang, C.G., Liu, H.Z., 2015. Fate of ochratoxin A during wheat milling and some Chinese breakfast processing. Food Control 57, 142–146.
Pfohl-Leszkowicz, A., Manderville, R.A., 2007. Ochratoxin A: an overview on toxicity and carcinogenicity in animals and humans. Mol. Nutr. Food Res. 51, 61–99.
Pinti, M., Gibellini, L., Liu, Y.Z., Xu, S., Lu, B., Cossarizza, A., 2015. Mitochondrial Lon protease at the crossroads of oxidative stress, ageing and cancer. Cell. Mol. Life Sci. 72, 4807–4824.
Pockley, A.G., 2003. Heat shock proteins as regulators of the immune response. Lancet 362, 469–476.
Qi, X.Z., Yang, X., Chen, S.Y., He, X.Y., Dweep, H., Guo, M.Z., Cheng, W.H., Xu, W.T., Luo, Y.B., Gretz, N., Dai, Q., Huang, K.L., 2014a. Ochratoxin A induced early hepatotoxicity: new mechanistic insights from microRNA, mRNA and proteomic profiling studies. Sci. Rep. 4.
Qi, X.Z., Yu, T., Zhu, L.Y., Gao, J., He, X.Y., Huang, K.L., Luo, Y.B., Xu, W.T., 2014b. Ochratoxin A induces rat renal carcinogenicity with limited induction of oxidative stress responses. Toxicol. Appl. Pharmacol. 280, 543–549.
Raghubeer, S., Nagiah, S., Phulukdaree, A., Chuturgoon, A., 2015. The phytoalexin resveratrol ameliorates ochratoxin a toxicity in human embryonic kidney (HEK293) cells. J. Cell. Biochem. 116, 2947–2955.
Ray, M.S., Moskovich, O., Iosefson, O., Fishelson, Z., 2014. Mortalin/GRP75 binds to complement C9 and plays a role in resistance to complement-dependent cytotoxicity. J. Biol. Chem. 289, 15014–15022.
Reinsch, M., Topfer, A., Lehmann, A., Nehls, I., 2005. Determination of ochratoxin A in wine by liquid chromatography tandem mass spectrometry after combined anion-exchange/reversed-phase clean-up. Anal. Bioanal. Chem. 381, 1592–1595.
Rozenberg, P., Ziporen, L., Gancz, D., Saar-Ray, M., Fishelson, Z., 2018. Cooperation between Hsp90 and mortalin/GRP75 in resistance to cell death induced by complement C5b-9. Cell Death Dis. 9, 150.
Shen, X.L., Zhang, Y., Xu, W.T., Liang, R., Zheng, J.J., Luo, Y.B., Wang, Y., Huang, K.L., 2013. An iTRAQ-based mitoproteomics approach for profiling the nephrotoxicity mechanisms of ochratoxin A in HEK 293 cells. J. Proteomics 78, 398–415.
Siddarth, M., Datta, S.K., Mustafa, M., Ahmed, R.S., Banerjee, B.D., Kalra, O.P., Tripathi, A.K., 2014. Increased level of organochlorine pesticides in chronic kidney disease patients of unknown etiology: role of GSTM1/GSTT1 polymorphism. Chemosphere 96, 174–179.
Stacchiotti, A., Ricci, F., Rezzani, R., Volti, G.L., Borsani, E., Lavazza, A., Bianchi, R., Rodella, L.F., 2006. Tubular stress proteins and nitric oxide synthase expression in rat kidney exposed to mercuric chloride and melatonin. J. Histochem. Cytochem. 54, 1149–1157.
Starenki, D., Hong, S.K., Lloyd, R.V., Park, J.I., 2015. Mortalin (GRP75/HSPA9) upregulation promotes survival and proliferation of medullary thyroid carcinoma cells. Oncogene 34, 4624–4634.
Sun, W., Xing, B., Sun, Y., Du, X., Lu, M., Hao, C., Lu, Z., Mi, W., Wu, S., Wei, H., Gao, X., Zhu, Y., Jiang, Y., Qian, X., He, F., 2007a. Proteome analysis of hepatocellular carcinoma by two-dimensional difference gel electrophoresis: novel protein markers in hepatocellular carcinoma tissues. Mol. Cell. Proteom. 6, 1798–1808.
Sun, Y., Deng, X., Li, W., Yan, Y., Wei, H., Jiang, Y., He, F., 2007b. Liver proteome analysis of adaptive response in rat immediately after partial hepatectomy. Proteomics 7, 4398–4407.
Tan, S.K., Sahoo, M.K., Milligan, S.B., Taylor, N., Pinsky, B.A., 2017. Stability of Zika virus in urine: specimen processing considerations and implications for the detection of RNA targets in urine. J. Virol Methods 248, 66–70.
Wang, Z.Y., Gall, J.M., Bonegio, R.G.B., Havasi, A., Hunt, C.R., Sherman, M.Y., Schwartz, J.H., Borkan, S.C., 2011. Induction of heat shock protein 70 inhibits ischemic renal injury. Kidney Int. 79, 861–870.
Wanigasuriya, K.P., Peiris-John, R.J., Wickremasinghe, R., 2011. Chronic kidney disease of unknown aetiology in Sri Lanka: is cadmium a likely cause? BMC Nephrol. 12, 32.
World Health Organization, G., 2006. Safety evaluation of certain contaminants in food. Prepared by the sixty-fourth meeting of the joint FAO/WHO expert committee on food additives (JECFA). FAO Food Nutr. Pap. 82, 1–778.
Wu, L.L., Chiou, C.C., Chang, P.Y., Wu, J.T., 2004. Urinary 8-OHdG: a marker of oxidative stress to DNA and a risk factor for cancer, atherosclerosis and diabetics. Clin. Chim. Acta 339, 1–9.
Yang, X., Xu, W., Huang, K., Zhang, B., Wang, H., Zhang, X., Gong, L., Luo, Y., He, X., 2019. Precision toxicology shows that troxerutin alleviates ochratoxin A-induced renal lipotoxicity. FASEB J. 33, 2212–2227.
Yang, X.A., Liu, S., Huang, C.C., Wang, H.M., Luo, Y.B., Xu, W.T., Huang, K.L., 2017. Ochratoxin A induced premature senescence in human renal proximal tubular cells. Toxicology 382, 75–83.
Zaied, C., Bouaziz, C., Azizi, I., Bensassi, F., Chour, A., Bacha, H., Abid, S., 2011. Presence of ochratoxin A in Tunisian blood nephropathy patients. Exposure level to OTA. Exp. Toxicol. Pathol. 63, 613–618.
Zanic-Grubisic, T., Zrinski, R., Cepelak, I., Petrik, J., Radic, B., Pepeljnjak, S., 2000. Studies of ochratoxin A-induced inhibition of phenylalanine hydroxylase and its reversal by phenylalanine. Toxicol. Appl. Pharmacol. 167, 132–139.
Zhang, B., Shen, X.L., Liang, R., Li, Y., Huang, K., Zhao, C., Luo, Y., Xu, W., 2014. Protective role of the mitochondrial Lon protease 1 in ochratoxin A-induced cytotoxicity in HEK293 cells. J. Proteom. 101, 154–168.
Zhang, L., Long, J., Jiang, W., Shi, Y., He, X., Zhou, Z., Li, Y., Yeung, R.O., Wang, J., Matsushita, K., Coresh, J., Zhao, M.H., Wang, H., 2016a. Trends in chronic kidney disease in China. N. Engl. J. Med. 375, 905–906.
Zhang, L., Wang, H., Long, J., Shi, Y., Bai, K., Jiang, W., He, X., Zhou, Z., Wang, J., Wang, F., Huang, J.F., Zhao, M., 2017. China kidney disease network (CK-NET) 2014 annual data report. Am. J. Kidney Dis. 69, A4.
Zhang, Z.Q., Gan, F., Xue, H.X., Liu, Y.H., Huang, D., Khan, A.Z., Chen, X.X., Huang, K.H., 2016b. Nephropathy and hepatopathy in weaned piglets provoked by natural ochratoxin A and involved mechanisms. Exp. Toxicol. Pathol. 68, 205–213.
Zheng, P., Chen, Q., Tian, X., Qian, N., Chai, P., Liu, B., Hu, J., Blackstone, C., Zhu, D., Teng, J., Chen, J., 2018. DNA damage triggers tubular endoplasmic reticulum extension to promote apoptosis by facilitating ER-mitochondria signaling. Cell Res. 28, 833–854.
Zhu, L.Y., Yu, T., Qi, X.Z., Gao, J., Huang, K.L., He, X.Y., Luo, H.S., Xu, W.T., 2016. Limited link between oxidative stress and ochratoxin A-induced renal injury in an acute toxicity rat model. Toxins 8.